This is an open access article published under a Creative Commons Non-Commercial No Derivative Works (CC-BY-NC-ND) Attribution License, which permits copying and redistribution of the article, and creation of adaptations, all for non-commercial purposes.

ACS AuthorChoice

Environmental Science & Technology

Article

pubs.acs.org/est

Iron Nanoparticle-Induced Activation of Plasma Membrane H$^+$-ATPase Promotes Stomatal Opening in *Arabidopsis thaliana*

Jae-Hwan Kim,[†] Youngjun Oh,[‡] Hakwon Yoon,[†] Inhwan Hwang,[‡] and Yoon-Seok Chang*[,†]

[†]School of Environmental Science and Engineering, and [‡]Division of Integrative Biosciences and Biotechnology, Pohang University of Science and Technology (POSTECH), Pohang 790-784, Republic of Korea

ABSTRACT: Engineered nanomaterials (ENMs) enable the control and exploration of intermolecular interactions inside microscopic systems, but the potential environmental impacts of their inevitable release remain largely unknown. Plants exposed to ENMs display effects, such as increase in biomass and chlorophyll, distinct from those induced by exposure to their bulk counterparts, but few studies have addressed the mechanisms underlying such physiological results. The current investigation found that exposure of *Arabidopsis thaliana* to nano zerovalent iron (nZVI) triggered high plasma membrane H$^+$-ATPase activity. The increase in activity caused a decrease in apoplastic pH, an increase in leaf area, and also wider stomatal aperture. Analysis of gene expression indicated that the levels of the H$^+$-ATPase isoform responsible for stomatal opening, *AHA2*, were 5-fold higher in plants exposed to nZVI than in unexposed control plants. This is the first study to show that nZVI enhances stomatal opening by inducing the activation of plasma membrane H$^+$-ATPase, leading to the possibility of increased CO_2 uptake.

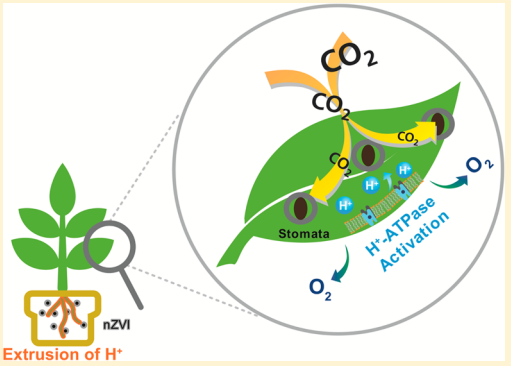

INTRODUCTION

Engineered nanomaterials (ENMs) currently used in a variety of industrial fields can be generally divided into four categories, as follows: (i) carbon-based materials, (ii) metal-based materials, (iii) dendrimers, and (iv) micrometer-sized composites with nanoparticles.[1] A number of products containing ENMs are readily available in the marketplace, including catalysts, electronics, personal care products, and medical devices.[2−4] Such applications of ENMs in commercial products are expected to gradually advance and directly or indirectly influence our way of life; however, as it is unknown whether they have a toxic effect on components of ecosystems and the increasing production and extensive use of commercially available ENMs has raised environmental concerns. ENMs such as Ag nanoparticles reduce the ATP content of human lung cells, and Mn_3O_4 nanoparticles increase reactive oxygen species production in the same cell type.[5,6]

The toxicity of ENMs to living organisms remains largely uncertain, however. In a study of metal-based ENMs, Fe_3O_4 nanoparticles had pH-dependent catalase- or peroxidase-like effects on human glioma cells and detoxified hydrogen peroxide into water and oxygen at neutral pH.[7] Studies of the effects of metal-based ENMs on plants have been species-specific and ambiguous, and this needs to be resolved. Ag nanoparticles inhibited germination in barley (*Hordeum vulgare*),[8] whereas those of Fe_3O_4 retarded root elongation of *Arabidopsis* (*Arabidopsis thaliana*), respectively.[9] In contrast, Fe_3O_4 nanoparticles increased the chlorophyll content of soybean leaves,[10] and low doses (0.01−0.05 mg/L) of Ag nanoparticles promoted soybean growth.[11]

The unique properties of nanoparticles, which include their reactivity and size, have produced outstanding improvements in the field of environmental remediation.[2,12−15] Nano zerovalent iron (nZVI) is a highly commercialized groundwater remediation reagent. Recently, investigation of the physiological changes of plants exposed to nZVI has been an important topic in environmental research. We previously demonstrated that it enhances root elongation in *Arabidopsis* by generating OH radicals and leading to the degradation of polysaccharides in the cell walls.[16] This was the first study to describe the mechanism underlying nZVI-mediated increase in root length in plants; however, because the rising scale of remediation has increased nZVI production, more information on the subsequent impacts of nZVI on plants is required.[17−20]

Plants respond to various external stimuli by extruding active agents into their environment; therefore, nZVI released into a plant's rhizosphere can be considered an external stimulus.[9,21] In particular, the strong oxidizing capacity of nZVI alters the pH by producing OH^- and this consequently leads to lower solubility of Fe ions in the rhizosphere.[22,23] Moreover, because the surface of nZVI consists of several iron oxide−hydroxides,[24] it is difficult for plants to use the particles as an iron source directly in the absence of Fe ion-reductase or any acidifiers.[25−27] Plants activate plasma membrane (PM) H$^+$-ATPase to extrude protons and acidify their rhizosphere, and thus increased activity of PM H$^+$-ATPase is frequently observed

Received: September 5, 2014
Revised: December 10, 2014
Accepted: December 12, 2014
Published: December 12, 2014

Downloaded via POHANG UNIV OF SCIENCE & TECHNOLOGY on July 16, 2019 at 07:49:37 (UTC).
See https://pubs.acs.org/sharingguidelines for options on how to legitimately share published articles.

 © 2014 American Chemical Society

DOI: 10.1021/es504375t
Environ. Sci. Technol. 2015, 49, 1113−1119

in plants growing in conditions of low Fe-availability.[25−27] Santi and Schmidt found that of the different PM H^+-ATPase isoforms, *Arabidopsis H⁺-ATPase 2* (*AHA2*) is the major Fe-responsive gene for rhizosphere acidification.[25]

It is well-known that the stomatal opening on leaves can be promoted by activation of PM H^+-ATPase.[28−31] Recent research into the effects of well-known components (including blue light receptors, plasma membrane H^+-ATPase, and K^+_{in} channel) regulating light-induced stomatal opening showed *AHA2* to be the major gene related to the stomatal opening process.[28] It is notable that *AHA2*, the PM H^+-ATPase isoform gene responsible for rhizosphere acidification, is identified as an essential component of stomatal opening. We therefore hypothesized that the presence of nZVI in rhizosphere would increase PM H^+-ATPase activity in plants and thus enhance the stomatal opening. To the best of our knowledge, no study has addressed both these phenomena together or considered the effects of ENMs on PM H^+-ATPase activation.

We measured sequentially the apoplastic pH in roots and the activity of PM H^+-ATPase in shoot. In addition, as the stoma is the key organ for CO_2 uptake for photosynthesis in plants, understanding how the stomatal opening is mediated by the activation of PM H^+-ATPase by nZVI may be useful in developing green technology to remove atmospheric CO_2.

MATERIALS AND METHODS

Experimental Engineered Nanomaterial. Commercial RNIP-10DS (Toda, Japan) was used as representative of nZVI in this study. An X-ray diffraction (XRD) pattern was recorded on a PANalytical X'Pert diffractometer (Cu Kα radiation) with an X'Celerator detector, and a transmission electron microscope (TEM) image was obtained by using JEOL-2100 high-resolution TEM (HR-TEM) with Cs correction at 200 kV. Surface area was measured by N_2 adsorption method using a Mirae SI nanoPorosity-XG analyzer. The average particle size and content of Fe^0 (α-Fe) in nZVI were calculated using Scherrer's formula with full width at half-maximum (fwhm)[32] (fwhm = 0.28°, 2θ = 44.6°) and using a gas chromatography thermal conductivity detector (GC-TCD),[24] respectively.

Plant Growth Conditions. To prepare the nZVI slurry, the particles were washed and rinsed with 99% ethanol and degassed deionized water.

I. Hydroponic Culture. A half strength of standard Murashige and Skoog medium (1/2 MS medium; Duchefa Biochemie) was used. The concentration of additives such as sucrose (Duchefa Bichemie), MES (aMResco), and agar (Junsei) were 20, 0.05, and 0.9%, respectively. A 70% ethanol and 20% Clorox solution was prepared to sterilize *Arabidopsis thaliana* (Colombia ecotype) seeds and the remainder of the procedure was described in more detail in aprevious work.[16] The concentration of nZVI used was 0.1 g/L. Growth chamber conditions were 16 h/8 h light/dark and 22 °C with 30% relative humidity. The measurement of leaf area and apoplastic pH of plants was conducted using *Arabidopsis* grown on the 1/2 MS medium. Using plants grown in medium, the measurements of apoplastic pH, leaf area, and expression of *AHA2* were conducted.

ii. Soil Culture. Autoclaved soil and nZVI slurry were mixed together to prepare nZVI mixed soil. The final concentration of nZVI to soil was 0.5 g/kg. *Arabidopsis* was cultivated on the soil and grown in the greenhouse with 16 h/8 h light/dark and at 20−22 °C. The initial water content of the nZVI mixed soil was 60−70%. Using plants grown in soil, the remainder of experiments as follows was conducted; PM H^+-ATPase activity, stomatal aperture, and water loss.

Measurement of Apoplastic pH in Roots. The 10-day-old seedlings were harvested and immersed in 0.005% bromocresol purple solutions (Sigma-aldrich) pH indicator containing 1/2 MS medium solution without agar for 2 days. The initial pH of the indicator solution for control and nZVI exposed seedlings were different, which were pH 5.8 and pH 6.0, respectively. The solution for nZVI exposed seedlings contained the same concentration of nZVI (0.1 g/L) to reflect the same condition of the rhizosphere in actual plates.

Stomatal Aperture Measurement. Stomatal apertures of 3-week-old seedlings grown in soil were measured as described by Hwang et al. with some modifications.[33] For this assay, any buffers such as K^+-MES that was able to stimulate stomatal opening were not used at all since the purpose of this assay was the comparison of the present state of stomatal apertures sizes when exposed to nZVI. Epidermal tissues were placed on a microscope slide and covered, and stomatal apertures were measured microscopically (Zeiss Axioplan). Statistical analysis was carried out using the Excel program (Microsoft Corp.).

Preparation of Plasma Membranes. Three-week-old plants were used to isolate protoplasts following a previous study.[34] The protoplasts were pelleted by centrifugation at 500 rpm for 4 min and then resuspended in 5 mL of lysis buffer (0.25 M sucrose, 1 mM EDTA, 20 mM Tris-HCl, pH 7.8). The protoplasts were homogenized by filter gently three times with two layered 11 μm pore nylon filters (Millipore). The extracts were centrifuged at 1000*g* for 10 min to remove chloroplasts and nuclear membranes. Supernatants were layered on 6 mL of 30% Percoll in lysis buffer and the centrifugation was performed at 28 000 rpm for 30 min in a Beckman ultracentrifuge with SW41Ti rotor. The plasma membrane fraction was visible as a ring shape in the ultracentrifuge tube and collected. The removal of Percoll was carried out by dilution with reaction buffer A (30 mM imidazole-HCl pH 7.4, 130 mM NaCl, 20 mM KCl, 4 mM $MgCl_2$). Next, 2 h of ultracentrifugation at 30 000 rpm was performed. Finally, 150 μL of supernatant was obtained by a 10 kDa cutoff centricon (Millipore).

Measurement of PM H^+-ATPase Activity. Plasma membrane (PM) H^+-ATPase activity was measured at 23 °C for 10 min with 10−20 μg of plasma membrane proteins. To reveal the pumping out activity of PM H^+-ATPase, 0.05% Brij 58 (Sigma) was employed to select inside-out vesicles. Reaction buffer B (30 mM imidazole-HCl pH 7.4, 4 mM $MgCl_2$, 2 mM sodium orthovanadate, 0.05% Brij 58) was used to eliminate the background signal of the ATPase activity. The 1 mL mixture of plasma membrane fraction with reaction buffer A, B was incubated on ice in the dark for 1 h. The addition of 4 mM Tris-ATP was the start cue of this assay. After 23 °C incubation for 10 min, the reaction was terminated by 100 μL of 20% SDS. To develop color as the activity reporter, 500 μL of the reaction mixture was added to 500 μL of reagent A which consisted of 3% ascorbic acid, 0.5 N HCl, and 0.5% ammonium molybdate and incubated on ice for 10 min. A 37 °C incubation for 10 min was performed, after the insertion of 500 μL of reagent B (2% sodium meta-arsenite, 2% trisodium citrate, 2% acetic acid) to 500 μL of reaction mixture and activity was detected by 850 nm wavelength.

Confocal Microscopy for Analysis of Endocytosis. We modified little the previous method from Kim et al.[16] From the two groups, 2-week-old seedlings were harvested and whole

DOI: 10.1021/es504375t
Environ. Sci. Technol. 2015, 49, 1113−1119

leaves, not only cuticle, were immersed in 1 μM of FM 4-64 solutions (Invitrogen) for 10 min. The emission and excitation wavelength employed for the fluorescence images were 543 nm and 560−615 nm, respectively (Zeiss Axioplan).

Quantitative Real-Time PCR (qRT-PCR). Total RNA was separately isolated from 2-week-old plants roots and leaves using a RNeasy plant mini kit (Qiagen). cDNA conversion was performed with cDNA reverse transcription kit (Biosystems). Quantitative real-time PCR (qRT-PCR) was carried out with a SYBR green kit to detect amplified probes. Actin 2 was empolyed as an endogeneous control. A 10 ng sample of cDNA was used to PCR in a 20 μL reaction volume with 0.5 μM primers, 1 unit Taq polymerase. Primer sequences are F 5′ TGACTGATCTTCGATCCTCTC 3′, R 5′GAGAATG-TGCATGTGCCAAAA 3′ for AHA2, F 5′ TATGAATTAC-CCGATGGGCAAG 3′, R 5′ TGGAACAAGACTTCTG-GGCAT 3′ for Actin 2. Amplification conditions were as follows: denaturation at 94 °C for 4 min, followed by 30 cycles at 94 °C for 15 s, 55 °C for 30 s, and 72 °C for 60 s.

RESULTS AND DISCUSSION

Characterization of Nano Zerovalent Iron. The chemicophysical properties of nZVI particles used, including the transmission electron microscopy (TEM) image, X-ray diffraction (XRD) pattern, surface area, particle size, and weight percentage (wt %) of Fe^0, are shown in Figure 1. Three peaks

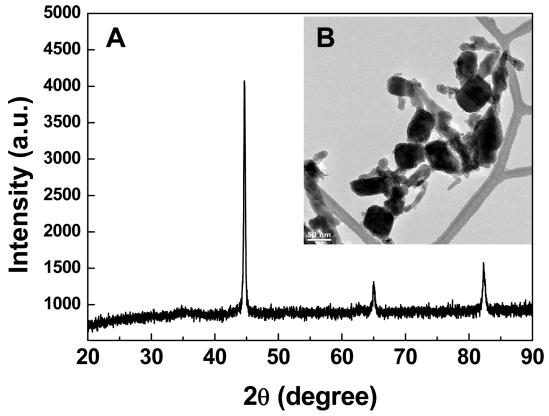

C

Surface area (m^2/g)	Particle size (nm)[a]	wt% of Fe^0 (%)[b]
30 ± 1	54 ± 1	40 ± 3

Figure 1. Chemicophysical properties of nano zerovalent iron particles used in the study. (A) X-ray diffraction (XRD) pattern; (B) transmission electron microscopy (TEM) image; (C) particle surface area, size, and weight percentage of Fe^0(α-Fe). (a) particle size was calculated using Scherrer's formula (2θ = 44.6°). (b) measurement of amount of H_2 evolution in concentrated HCl using GC-TCD. Scale bar in image B: 50 nm.

were present in the crystal at 44.6, 66.0, and 82.3°, indicating a typical Fe^0 XRD pattern (Figure 1A). The TEM image of nZVI is shown in Figure 1B. Single particles appeared to be less than 100 nm in size, but agglomeration of particles occurred due to chemical characteristics such as magnetic interaction and Van der Walls attractions.[35] The surface area was 30 ± 2 m^2/g, and the mean particle size (calculated using Sherrer's formula[32]) was 54 ± 1 nm (Figure 1C). The weight percent of Fe^0 in nZVI had a slightly higher value compared with an earlier analysis.[24]

nZVI Increases Plasma Membrane H^+-ATPase Activity. Two groups of 10-day-old seedlings, one treated with nZVI and the other an untreated control group, were incubated in bromoceresol purple solutions (0.005%) for 2 days to measure changes in the apoplastic pH. The densities of the solutions were quantitatively determined using UV spectrophotometry (Figure 2A). The negative value seen when *Arabidopsis*

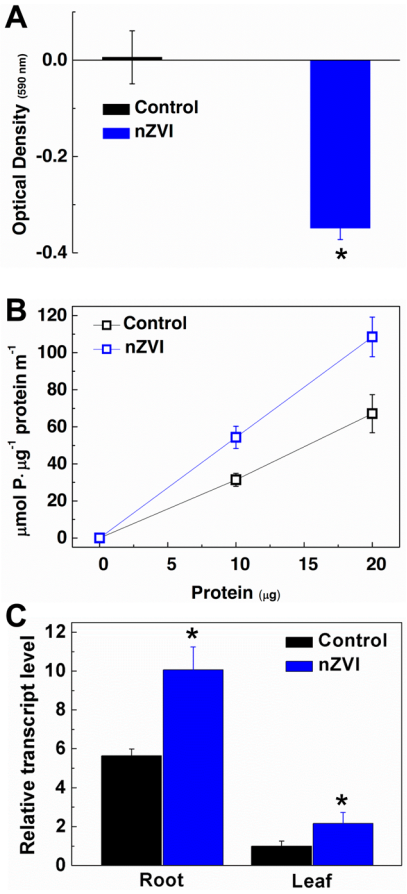

Figure 2. Effects of nano zerovalent iron (nZVI) on apoplastic pH, H^+-ATPase activity, and *AHA2* expression in *Arabidopsis thaliana*. (A) *In vivo* determination of the extrusion of protons. The 10-day-old *Arabidopsis* seedlings were incubated in bromocresol purple solutions for 2 days (n = 10, triplicate). (B) PM H^+-ATPase activity in 3-week-old *Arabidopsis* seedling. (C) Expression of *AHA2* in 2-week-old *Arabidopsis* seedlings. Data are mean and SE of three replicate experiments; n = 10 in each experiment. Untreated seedlings were used as controls in each experiment. The asterisk (∗) indicates statistically significant differences at $P < 0.01$ compared with the control (Student's t-test).

seedlings were exposed to nZVI indicated their apoplastic pH was more acidic than pH 5.8. By contrast, the apoplastic pH of control seedlings remained almost constant throughout the experiment; thus the apoplastic pH decreased following exposure to nZVI. This acidification of the root apoplast was correlated with an increase in PM H^+-ATPase activity. PM H^+-ATPase plays an important role in transporting protons[29,36,37] and, by pumping protons out of the roots, plants are able to acidify the rhizosphere when sparingly soluble metal ions such as iron are present.[25,26]

Nano zerovalent iron has unique redox reactivity. On exposure to aerobic conditions, insoluble iron oxide-hydroxides, such as FeOOH and $Fe(OH)_3$, form rapidly on the surface of

DOI: 10.1021/es504375t
Environ. Sci. Technol. 2015, 49, 1113−1119

each particle because of their strong oxidizing capacity.[24,38−40] Additionally, nZVI can thermodynamically lead to lower Fe solubility by increasing pH via water decomposition following electrochemical/corrosion reactions.[40] Together, these effects of nZVI reduce Fe availability in the rhizosphere, which enables the operation of the proton pump in plants.

$$Fe^{0}_{(s)} + 2H_2O_{(aq)} \rightarrow Fe^{2+/3+}_{(aq)} + H_{2(g)} + 2OH^{-}_{(aq)} \quad (1)$$

$$Fe^{3+}_{(aq)} + 3OH^{-} \rightarrow Fe(OH)_{3(s)} \quad (2)$$

$$Fe(OH)_{3(s)} \rightarrow FeOOH_{(s)} + H_2O \quad (3)$$

Therefore, the acidic apoplastic pH observed in *Arabidopsis* exposed to nZVI indicates that its presence may produce rhizosphere conditions requiring acidification, thereby triggering the activation of PM H^+-ATPase.

To determine whether PM H^+-ATPase increased in the guard cells of *Arabidopsis* exposed to nZVI, the activity of PM H^+-ATPase was directly measured in 3-week-old seedlings. Figure 2B shows PM H^+-ATPase activity of the experimental and control plants. Plants exposed to nZVI exhibited much higher levels (an 80−90% increase) of PM H^+-ATPase activity in their aerial part than the control plants, which implies that nZVI triggered activation of PM H^+-ATPase across the whole plant, possibly due to cross-talk between PM H^+-ATPase and auxin.[36,41,42]

The roots and shoots exchange signals to perform communication with each other.[43] Activation of PM H^+-ATPase can be mediated by auxin, which is the most important signal transmitted from root to shoot; PM H^+-ATPase activation is likewise required for auxin transport.[41] A chemiosmotic model[44] suggests that intercellular transport of auxin is accelerated while the PM H^+-ATPase channel, through which protons are pumped out, is open ("activated"). This provides a possible mechanism by which PM H^+-ATPase activity could increase in the shoots of *Arabidopsis* exposed to nZVI, and suggests that such exposure promotes the transport of auxin from root to shoot. Therefore, the activation of PM H^+-ATPase in roots by nZVI promotes auxin transport, in accordance with the chemiosmotic model of polar auxin transport, which may lead to activation of PM H^+-ATPase in shoots.

The quantitative real-time polymerase chain reaction was used to analyze the levels of *AHA2* (the major H^+-ATPase isoform involved in rhizosphere acidification)[25] and thus specifically evaluate PM H^+-ATPase expression at the transcriptional level. The increased expression of *AHA2* in the roots of plants exposed to nZVI (Figure 2C) clearly supports the hypothesis that nZVI induces the need to acidify the rhizosphere.

Increased Stomatal Aperture and Tolerance to Drought. These observations led us to hypothesize that any increase in stomatal aperture observed following exposure of plants to nZVI would result from the activation of PM H^+-ATPase in leaves. Guard cells swell due to a K^+ or Na^+ influx through inward-rectifying channels and the stomata open when PM H^+-ATPase in guard cells is activated.[45] Recently, *AHA2* was found to have another role in leaves as a key component in stomatal opening,[28] in addition to being the major Fe-responsive PM H^+-ATPase isoform in roots.[25] *AHA2* levels increased almost 2-fold not only in roots but also in leaves of *Arabidopsis* exposed to nZVI (Figure 2C).

Wang et al. evaluated the function of *AHA2*, as well as other factors associated with light-induced stomatal opening, such as blue light receptor phototropin 2 (PHOT2) and PM inward-rectifying K^+_{in} channels (KAT1, AKT1,).[28] The stomatal aperture was increased only by activation of PH H^+-ATPase in transgenic *Arabidopsis* overexpressing *AHA2*:[28] the stomatal aperture of transgenic plants were approximately 25% wider under light condition, and the expression of *AHA2* was 3.4 to 5.2-fold higher; thus we predicted that stomatal apertures would also increase in *Arabidopsis* exposed to nZVI due to their higher levels of *AHA2*.

To confirm this, the sizes of stomatal apertures in the two groups of plants were measured. Figure 3 shows images of

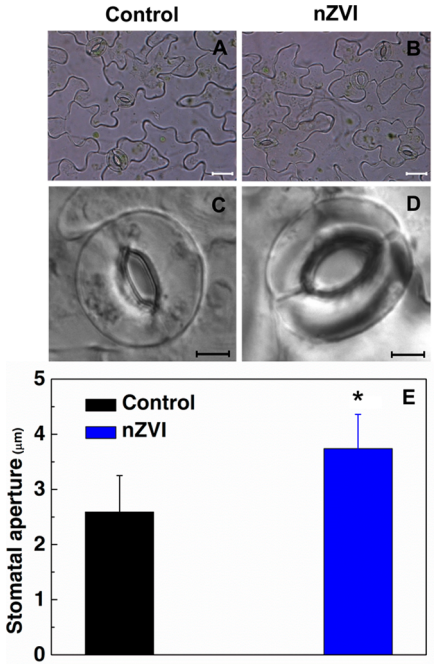

Figure 3. The effect of nano zerovalent iron (nZVI) on the stomatal aperture in *Arabidopsis thaliana*. (A−D) Confocal microscopy images, taken at low and high magnification, of guard cells in 3-week-old seedling. (A and C) control seedlings. (B and D) nZVI-exposed seedlings. White scale bars: 20 μm. Black scale bars: 5 μm. (E) The average stomatal apertures of control and nZVI-exposed seedling. Data are means and SE of three replicate experiment; n = 20 in each experiment. The asterisk (∗) indicates statistically significant differences at $P < 0.01$ compared with the control (Student's t-test).

Arabidopsis guard cells. The average size of the stomatal aperture of plants exposed to nZVI (3.7 ± 0.6 μm) was larger than that of the control (2.6 ± 0.7 μm). These results corresponded with higher activation of PM H^+-ATPase in plants exposed to nZVI (Figure 2B) and thus supported our hypothesis. Therefore, we concluded that the enhanced stomatal opening was induced by the activation of PM H^+-ATPase by nZVI. Together with our earlier study, the finding of strong induction in AHA2 expression (Figure 2C) may answer the fundamental question of how exposure to nZVI increases the stomatal aperture of *Arabidopsis*. This is the first study not only to consider the effects of ENMs on PM H^+-ATPase activation but also aspects of dual roles of *AHA2* in roots and leaves.

Although *AHA2*-transgenic plants have wider stomatal apertures than wild-type plants, they show a normal drought

DOI: 10.1021/es504375t
Environ. Sci. Technol. 2015, 49, 1113−1119

response in darkness and in response to the hormone abscisic acid.[28] *AHA2*-overexpressing *Arabidopsis* exposed to nZVI are expected to have similar responses. To determine whether *Arabidopsis* exposed to nZVI exhibit a normal drought response, a water-loss experiment was performed using detached rosette leaves.

The kinetics of weight decrease in detached rosette leaves from the treated and control plants were very similar (Figure 4), consistent with the behavior of *AHA2*-transgenic plants

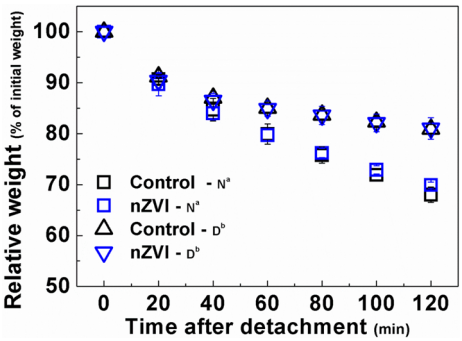

Figure 4. Water loss from detached rosette leaves of 4-week-old *Arabidopsis thaliana*. The *Y*-axis relative weight is presented as a percentage of the initial fresh weight. The fresh weight of the detached leaves was measured at the indicated time points. (a) N, normal humidity; (b) D, relatively low humidity.

reported previously.[28] Despite the wider opening of stomata following exposure to nZVI, the rates of water loss were nearly identical under conditions of both normal humidity and dehydration, indicating that the plants exposed to nZVI retained normal sensitivity and the ability to close stomata upon dehydration. The observation that *Arabidopsis* with nZVI-mediated activation of PM H^+-ATPase showed not only increased stomatal opening but also normal drought sensitivity raises the possibility that these plants may have an increased CO_2 assimilation rate and respond normally to diverse environmental changes. Enhancement of the CO_2 assimilation rate by plants through manipulation of their stomatal movements has been proposed as an eco-friendly alternative approach to reduce CO_2 and thus combat climate change.[28,46]

PM H^+-ATPase and Enlarged Leaf Area. *Arabidopsis* seedlings were grown for 14 days in 1/2 MS medium with control conditions or nZVI mixed conditions (Figure 5A–D). The surface areas of the leaves were quantified after 2 and 3 weeks growth. The leaf area of *Arabidopsis* seedlings exposed to nZVI was approximately 50% larger than that of the control plants (Figure 5E). Some ENMs, such as Ag nanoparticles, are known to increase biomass.[11] While evaluating the toxic effects of various concentrations of silver nanoparticles on *Arabidopsis*, Wang et al. found that a relatively low dose (0.05 mg/L) of silver nanoparticles increased root elongation and leaf area. They speculated that the enhancement of root elongation was caused by Ag ions released from Ag nanoparticles, which might cause changes to levels of phytohormones or induce hormesis; however, they did not provide any clear evidence or mechanism to explain how low-dose silver nanoparticle treatment increased the leaf area.[11]

Activation of PM H^+-ATPase is involved in cell-wall loosening,[31,36,45] which is necessary for various aspects of plant development including elongation, ripening, and expansion.[30] An increased level of PM H^+-ATPase causes

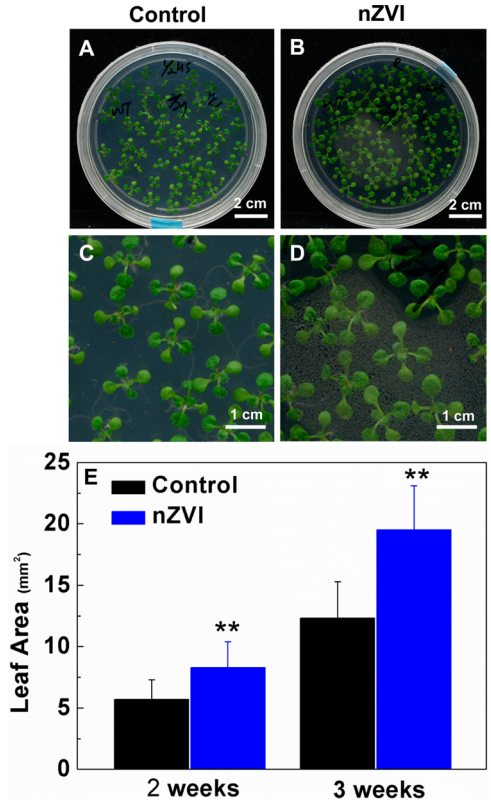

Figure 5. Effects of nano zerovalent iron (nZVI) on leaf. *Arabidopsis thaliana* seedlings were grown for 2 weeks and photographed under low and high magnification. (A and C) control seedlings. (B and D) nZVI-exposed seedlings. (E) Leaf areas of control and nZVI-exposed seedlings measured after 2 and 3 weeks. Data are means and SE of three replicate experiments; n = 40 in each experiment. The double asterisk (**) indicates statistically significant differences at $P < 0.001$, compared with the control (Student's t-test).

more protons to be pumped across the PM, resulting in acidification of the apoplast. The acidic conditions activate pH-sensitive proteins and enzymes such as expansins,[47] xyloglucan hydrolase, xyloglucan endotransglycosylase,[48] and yieldins,[49] which cause the acid-induced extension of cell walls. Expansins are known to disrupt the hydrogen bonding that connects glycans and cellulose microfibril in the cell–wall matrix without degrading the cellulose, therefore allowing the slippage of cellulose microfibrils during expansion. Their activity increases with pH between pH 4.5 and 6.[30] Hydrolysis of molecules between adjacent cellulose filaments and other polysaccharides in cell walls by these proteins and enzymes eventually leads to turgor-driven cell expansion.[30]

To determine if leaf expansion was mediated by turgor-driven cell elongation, we compared the endocytosis rates of leaves from the two groups of plants, because turgor-driven cell-wall loosening is inversely correlated with the endocytosis rate. Figure 6 shows leaf cells stained with FM 4–64 dye, an endocytosis marker. The rate of endocytosis clearly differed between the two groups of leaves, being lower in nZVI-treated leaves. The endocytosis rate is regulated according to the degree of tension on cell walls. Cell expansion via turgor-driven cell-wall loosening increases the tension on cell walls and consequently inhibits endocytosis and facilitates exocytosis.[50,51] The reduction in endocytosis seen in leaves of nZVI-treated seedlings (Figure 6) supports our hypothesis that leaf expansion occurred via turgor-driven cell-wall loosening. This

DOI: 10.1021/es504375t
Environ. Sci. Technol. 2015, 49, 1113–1119

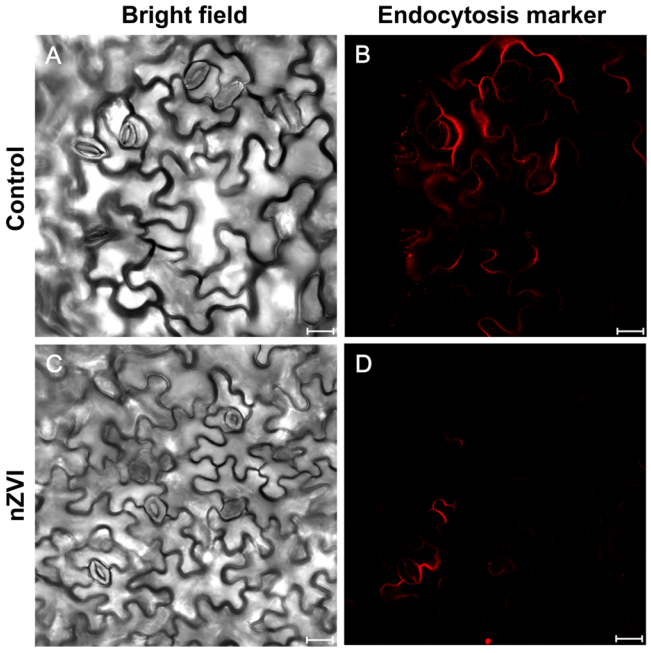

Figure 6. Effect of nano zerovalent iron (nZVI) on endocytosis in *Arabidopsis thaliana*. Images of leaf cells from control and nZVI-treated plants. Bright field (leaf column) and red channel (right column) images of leaf cells strained with the endocytosis marker FM 4-64 from control (top) and nZVI-exposed (bottom) seedlings. Two-week-old seedlings were incubated in 1 μM FM 4-64 for 10 min. Scale bars: 20 μm.

would mean the enlarged leaf area of nZVI-treated plants resulted from an increased extrusion of protons into the apoplast due to the increased levels of PM H^+-ATPase; thus the pH of the apoplast is lowered, producing the acidic conditions that allow turgor-driven cell-wall loosening.

Environmental Implications. In the global ecosystem, one of the most important roles of plants is providing O_2 while absorbing CO_2. In higher plants, O_2 and CO_2 are exchanged in the stomata and, therefore, much attention has been paid to the development and application of advanced technologies that modulate stomatal aperture. In this context, the regulation of PM H^+-ATPase activity is of particular interest.[29,36,37,52,53] An earlier study reported the response of stomata to ENMs, showing that Ag nanoparticles caused stomatal closure by decreasing hydraulic conductance of stems after penetrating into vessel; however, that study focused only on postharvest technology,[54] and thus it is not directly relevant to the release of nanoparticles into the environment. Here, it was shown that *Arabidopsis* plants exposed to nZVI exhibited higher levels of *AHA2* expression as well as higher PM H^+-ATPase activity, and showed behavior similar to that of transgenic plants over-expressing *AHA2*,[28,29,45] at least in terms of the water loss and stomatal aperture. These results, therefore, raise the possibility of an eco-friendly alternative approach to CO_2 reduction. For this to be applied, however, it will be necessary to characterize in detail the plant's responses to nZVI exposure, including its effects on the rate of CO_2 assimilation, biomass production, and photosynthesis.

AUTHOR INFORMATION

Corresponding Author

*Phone: +82-54-279-2281; fax: +82-54-279-8299; e-mail: yschang@postech.ac.kr.

Notes

The authors declare no competing financial interest.

ACKNOWLEDGMENTS

We thank Eun-jung Lee under Prof. Youngsook Lee (POSTECH) for the microscopy analysis of stomata. This work was supported by the National Research Foundation of Korea (NRF) grant funded by the Korea government (MEST) (No. 2011-0028723) and "The GAIA Project" by the Korea Ministry of Environment.

REFERENCES

(1) Stampoulis, D.; Sinha, S. K.; White, J. C. Assay-dependent phytotoxicity of nanoparticles to plants. *Environ. Sci. Technol.* **2009**, *43*, 9473−9479.

(2) Kim, J. H.; Tratnyek, P. G.; Chang, Y. S. Rapid dechlorination of polychlorinated dibenzo-*p*-dioxins by bimetallic and nanosized zerovalent iron. *Environ. Sci. Technol.* **2008**, *42*, 4106−4112.

(3) Weir, A.; Westerhoff, P.; Fabricius, L.; Hristovski, K.; Von Goetz, N. Titanium dioxide nanoparticles in food and personal care products. *Environ. Sci. Technol.* **2012**, *46*, 2242−2250.

(4) Duan, X.; Fu, T. M.; Liu, J.; Lieber, C. M. Nanoelectronics-biology frontier: From nanoscopic probes for action potential recording in live cells to three-dimensional cyborg tissues. *Nano Today* **2013**, *8*, 351−373.

(5) Limbach, L. K.; Wick, P.; Manser, P.; Grass, R. N.; Bruinink, A.; Stark, W. J. Exposure of engineered nanoparticles to human lung epithelial cells: Influence of chemical composition and catalytic activity on oxidative stress. *Environ. Sci. Technol.* **2007**, *41*, 4158−4163.

(6) AshaRani, P. V.; Mun, G. L. K.; Hande, M. P.; Valiyaveettil, S. Cytotoxicity and genotoxicity of silver nanoparticles in human cells. *ACS Nano* **2009**, *3*, 279−290.

(7) Chen, Z.; Yin, J. J.; Zhou, Y. T.; Zhang, Y.; Song, L.; Song, M.; Hu, S.; Gu, N. Dual enzyme-like activities of iron oxide nanoparticles and their implication for diminishing cytotoxicity. *ACS Nano* **2012**, *6*, 4001−4012.

(8) El-Temsah, Y. S.; Joner, E. J. Impact of Fe and Ag nanoparticles on seed germination and differences in bioavailability during exposure in aqueous suspension and soil. *Environ. Toxicol.* **2012**, *27*, 42−49.

(9) Lee, C. W.; Mahendra, S.; Zodrow, K.; Li, D.; Tsai, Y. C.; Braam, J.; Alvarez, P. J. J. Developmental phytotoxicity of metal oxide nanoparticles to Arabidopsis thaliana. *Environ. Toxicol. Chem.* **2010**, *29*, 669−675.

(10) Ghafariyan, M. H.; Malakouti, M. J.; Dadpour, M. R.; Stroeve, P.; Mahmoudi, M. Effects of magnetite nanoparticles on soybean chlorophyll. *Environ. Sci. Technol.* **2013**, *47*, 10645−10652.

(11) Wang, J.; Koo, Y.; Alexander, A.; Yang, Y.; Westerhof, S.; Zhang, Q.; Schnoor, J. L.; Colvin, V. L.; Braam, J.; Alvarez, P. J. J. Phytostimulation of poplars and Arabidopsis exposed to silver nanoparticles and Ag+ at sublethal concentrations. *Environ. Sci. Technol.* **2013**, *47*, 5442−5449.

(12) Kim, E. J.; Le Thanh, T.; Kim, J. H.; Chang, Y. S. Synthesis of metal sulfide-coated iron nanoparticles with enhanced surface reactivity and biocompatibility. *RSC Adv.* **2013**, *3*, 5338−5340.

(13) Gunawardana, B.; Singhal, N.; Swedlund, P. Degradation of chlorinated phenols by zero valent iron and bimetals of iron: A review. *Environ. Eng. Res.* **2011**, *16*, 187−203.

(14) Saleh, N.; Sirk, K.; Liu, Y.; Phenrat, T.; Dufour, B.; Matyjaszewski, K.; Tilton, R. D.; Lowry, G. V. Surface modifications enhance nanoiron transport and NAPL targeting in saturated porous media. *Environ. Eng. Sci.* **2007**, *24*, 45−57.

(15) Roco, M. C. Environmentally responsible development of nanotechnology. *Environ. Sci. Technol.* **2005**, *39*, 106A−112A.

(16) Kim, J. H.; Lee, Y.; Kim, E. J.; Gu, S.; Sohn, E. J.; Seo, Y. S.; An, H. J.; Chang, Y. S. Exposure of iron nanoparticles to Arabidopsis thaliana enhances root elongation by triggering cell wall loosening. *Environ. Sci. Technol.* **2014**, *48*, 3477−3485.

DOI: 10.1021/es504375t
Environ. Sci. Technol. 2015, 49, 1113−1119

(17) Kanel, S. R.; Greneche, J. M.; Choi, H. Arsenic(V) removal from groundwater using nano scale zero-valent iron as a colloidal reactive barrier material. *Environ. Sci. Technol.* **2006**, *40*, 2045−2050.
(18) Li, X. Q.; Elliott, D. W.; Zhang, W. X. Zero-valent iron nanoparticles for abatement of environmental pollutants: Materials and engineering aspects. *Crit. Rev. Solid State* **2006**, *31*, 111−122.
(19) Tratnyek, P. G.; Johnson, R. L. Nanotechnologies for environmental cleanup. *Nano Today* **2006**, *1*, 44−48.
(20) Phenrat, T.; Saleh, N.; Sirk, K.; Tilton, R. D.; Lowry, G. V. Aggregation and sedimentation of aqueous nanoscale zerovalent iron dispersions. *Environ. Sci. Technol.* **2007**, *41*, 284−290.
(21) Miralles, P.; Church, T. L.; Harris, A. T. Toxicity, uptake, and translocation of engineered nanomaterials in vascular plants. *Environ. Sci. Technol.* **2012**, *46*, 9224−9239.
(22) Sharma, V. K.; MácOvá, Z.; Bouzek, K.; Millero, F. J. Solubility of ferrate(VI) in NaOH−KOH mixtures at different temperatures. *J. Chem. Eng. Data* **2010**, *55*, 5594−5597.
(23) Cameron, F. K.; Bell, J. M.; Robinson, W. O. The solubility of certain salts present in alkali soils. *J. Phys. Chem.* **1907**, *11*, 396−420.
(24) Liu, Y.; Majetich, S. A.; Tilton, R. D.; Sholl, D. S.; Lowry, G. V. TCE dechlorination rates, pathways, and efficiency of nanoscale iron particles with different properties. *Environ. Sci. Technol.* **2005**, *39*, 1338−1345.
(25) Santi, S.; Schmidt, W. Dissecting iron deficiency-induced proton extrusion in Arabidopsis roots. *New Phytol.* **2009**, *183*, 1072−1084.
(26) Dell'Orto, M.; Santi, S.; De Nisi, P.; Cesco, S.; Varanini, Z.; Zocchi, G.; Pinton, R. Development of Fe-deficiency responses in cucumber (*Cucumis sativus* L.) roots: Involvement of plasma membrane H+-ATPase activity. *J. Exp. Bot.* **2000**, *51*, 695−701.
(27) Ohwaki, Y.; Sugahara, K. Active extrusion of protons and exudation of carboxylic acids in response to iron deficiency by roots of chickpea (*Cicer arietinum L.*). *Plant Soil* **1997**, *189*, 49−55.
(28) Wang, Y.; Noguchi, K.; Ono, N.; Inoue, S. I.; Terashima, I.; Kinoshita, T. Overexpression of plasma membrane H+-ATPase in guard cells promotes light-induced stomatal opening and enhances plant growth. *Proc. Natl. Acad. Sci. USA* **2014**, *111*, 533−538.
(29) Hashimoto-Sugimoto, M.; Higaki, T.; Yaeno, T.; Nagami, A.; Irie, M.; Fujimi, M.; Miyamoto, M.; Akita, K.; Negi, J.; Shirasu, K.; Hasezawa, S.; Iba, K. A Munc13-like protein in Arabidopsis mediates H+-ATPase translocation that is essential for stomatal responses. *Nat. Commun.* **2013**, *4*.
(30) Cosgrove, D. J. Growth of the plant cell wall. *Nat. Rev. Mol. Cell Biol.* **2005**, *6*, 850−861.
(31) Hager, A. Role of the plasma membrane H+-ATPase in auxin-induced elongation growth: Historical and new aspects. *J. Plant Res.* **2003**, *116*, 483−505.
(32) Sun, S.; Zeng, H. Size-controlled synthesis of magnetite nanoparticles. *J. Am. Chem. Soc.* **2002**, *124*, 8204−8205.
(33) Hwang, J. U.; Jeon, B. W.; Hong, D.; Lee, Y. Active ROP2 GTPase inhibits ABA- and CO 2-induced stomatal closure. *Plant Cell Environ.* **2011**, *34*, 2172−2182.
(34) Jin, J. B.; Kim, Y. A.; Kim, S. J.; Lee, S. H.; Kim, D. H.; Cheong, G. W.; Hwang, I. A new dynamin-like protein, ADL6, is involved in trafficking from the trans-Golgi network to the central vacuole in Arabidopsis. *Plant Cell* **2001**, *13*, 1511−1525.
(35) Jiang, Z.; Lv, L.; Zhang, W.; Du, Q.; Pan, B.; Yang, L.; Zhang, Q. Nitrate reduction using nanosized zero-valent iron supported by polystyrene resins: Role of surface functional groups. *Water Res.* **2011**, *45*, 2191−2198.
(36) Rober-Kleber, N.; Albrechtová, J. T. P.; Fleig, S.; Huck, N.; Michalke, W.; Wagner, E.; Speth, V.; Neuhaus, G.; Fischer-Iglesias, C. Plasma membrane H+-ATPase is involved in auxin-mediated cell elongation during wheat embryo development. *Plant Physiol.* **2003**, *131*, 1302−1312.
(37) Yan, F.; Zhu, Y.; Müller, C.; Zörb, C.; Schubert, S. Adaptation of H+ -pumping and plasma membrane H+ ATPase activity in proteoid roots of white lupin under phosphate deficiency. *Plant Physiol.* **2002**, *129*, 50−63.
(38) Al-Shamsi, M. A.; Thomson, N. R. Treatment of organic compounds by activated persulfate using nanoscale zerovalent iron. *Ind. Eng. Chem. Res.* **2013**, *52*, 13564−13571.
(39) Sohn, K.; Kang, S. W.; Ahn, S.; Woo, M.; Yang, S. K. Fe(0) nanoparticles for nitrate reduction: Stability, reactivity, and transformation. *Environ. Sci. Technol.* **2006**, *40*, 5514−5519.
(40) Zhang, W. X. Nanoscale iron particles for environmental remediation: An overview. *J. Nanopart. Res.* **2003**, *5*, 323−332.
(41) Hohm, T.; Demarsy, E.; Quan, C.; Allenbach Petrolati, L.; Preuten, T.; Vernoux, T.; Bergmann, S.; Fankhauser, C. Plasma membrane H+-ATPase regulation is required for auxin gradient formation preceding phototropic growth. *Mole. Syst. Biol.* **2014**, *10*.
(42) Takahashi, K.; Hayashi, K. I.; Kinoshita, T. Auxin activates the plasma membrane H+-ATPase by phosphorylation during hypocotyl elongation in Arabidopsis. *Plant Physiol.* **2012**, *159*, 632−641.
(43) Ko, D.; Kang, J.; Kiba, T.; Park, J.; Kojima, M.; Do, J.; Kim, K. Y.; Kwon, M.; Endler, A.; Song, W. Y.; Martinoia, E.; Sakakibara, H.; Lee, Y. Arabidopsis ABCG14 is essential for the root-to-shoot translocation of cytokinin. *Proc. Natl. Acad. Sci. USA* **2014**, *111*, 7150−7155.
(44) Taiz, L.; Zeiger, E. *Plant Physiology*, 5th ed.; Sinauer Associates: Sunderland, MA, 2010.
(45) Kinoshita, T.; Hayashi, Y. New insights into the regulation of stomatal opening by blue light and plasma membrane H +-ATPase. *Int. Rev. Cel. Mol. Biol.* **2011**, *289*, 89−115.
(46) Hetherington, A. M.; Woodward, F. I. The role of stomata in sensing and driving environmental change. *Nature* **2003**, *424*, 901−908.
(47) Cosgrove, D. J. How do plant cell walls extend? *Plant Physiol.* **1993**, *102*, 1−6.
(48) Fry, S. C.; Smith, R. C.; Renwick, K. F.; Martin, D. J.; Hodge, S. K.; Matthews, K. J. Xyloglucan endotransglycosylase, A new wall-loosening enzyme activity from plants. *Biochem. J.* **1992**, *282*, 821−828.
(49) Okamoto-Nakazato, A.; Nakamura, T.; Okamoto, H. The isolation of wall-bound proteins regulating yield threshold tension in glycerinated hollow cylinders of cowpea hypocotyl. *Plant Cell Environ.* **2000**, *23*, 145−154.
(50) Nakayama, N.; Smith, R. S.; Mandel, T.; Robinson, S.; Kimura, S.; Boudaoud, A.; Kuhlemeier, C. Mechanical regulation of auxin-mediated growth. *Curr. Biol.* **2012**, *22*, 1468−1476.
(51) Li, H.; Friml, J.; Grunewald, W. Cell polarity: Stretching prevents developmental cramps. *Curr. Biol.* **2012**, *22*, R635−R637.
(52) Shimazaki, K.; Iino, M.; Zeiger, E. Blue light-dependent proton extrusion by guard-cell protoplasts of vicia faba. *Nature* **1986**, *319*, 324−326.
(53) Assmann, S. M.; Simoncini, L.; Schroeder, J. I. Blue light activates electrogenic ion pumping in guard cell protoplasts of Vicia faba. *Nature* **1985**, *318*, 285−287.
(54) Lü, P.; Cao, J.; He, S.; Liu, J.; Li, H.; Cheng, G.; Ding, Y.; Joyce, D. C. Nano-silver pulse treatments improve water relations of cut rose cv. Movie star flowers. *Postharvest Biol. Technol.* **2010**, *57*, 196−202.

DOI: 10.1021/es504375t
Environ. Sci. Technol. 2015, 49, 1113−1119